RADIATION RESEARCH **163**, 591–602 (2005)
0033-7587/05 $15.00

Sugar Radicals in DNA: Isolation of Neutral Radicals in Gamma-Irradiated DNA by Hole and Electron Scavenging

Lata I. Shukla,[1] Robert Pazdro, David Becker and Michael D. Sevilla[2]

Department of Chemistry, Oakland University, Rochester, Michigan 48309

Shukla, L. I., Pazdro, R., Becker, D. and Sevilla, M. D. Sugar Radicals in DNA: Isolation of Neutral Radicals in Gamma-Irradiated DNA by Hole and Electron Scavenging. *Radiat. Res.* 163, 591–602 (2005).

In this investigation of the radical formation and the reaction of radicals in γ-irradiated DNA, we report the isolation of putative neutral radicals by the scavenging of holes by $Fe(CN)_6^{4-}$ and of electrons by $Fe(CN)_6^{3-}$. Experiments are performed under conditions that emphasize direct and quasi-direct effects (collectively called direct-type effects.) Samples containing $Fe(CN)_6^{4-}$ show effective scavenging of holes and the ESR spectra obtained arise principally from DNA anion radicals and neutral radicals. On the other hand, for samples containing $Fe(CN)_6^{3-}$, electron scavenging is highly efficient, and the resulting spectra arise principally from guanine cation radicals and neutral radicals. When both $Fe(CN)_6^{4-}$ and $Fe(CN)_6^{3-}$ are present, a near complete scavenging of cation radicals and anion radicals is observed at 77 K, and the ESR spectra that result originate predominantly with neutral radicals which are assigned predominantly to radicals on the sugar phosphate backbone. A notable finding is the presence of spectral components that indicate the formation, through the rupture of the C3′–O bond, of a neutral deoxyribose radical; a concurrent strand break must accompany formation of this radical. This radical was previously reported in argon-ion-irradiated DNA and now, for the first time, is reported in DNA irradiated with low-LET radiation.

INTRODUCTION

It is generally recognized that the biologically unrepairable double-strand break is a critical component of the damage to irradiated DNA (*1, 2*). In light of this, the nature of the reaction mechanisms that lead to strand breaks has become a topic of intense interest in DNA radiation chemistry. Free radicals located on the deoxyribose moiety are the likely precursors to strand breaks; the C1′• leads to an abasic site (*3*) and the C3′•, C4′• and C5′• lead to prompt strand breaks (*4*). ESR studies of irradiated DNA at low temperature indicate that about 85–90% of free radicals stabilized at 77 K are localized predominantly on the DNA bases (*5–7*). Because so few of the radicals stabilized are located on the sugar phosphate backbone, they have been difficult to identify and characterize.

Some of the earliest work on the radicals present in irradiated DNA at 77 K did not find evidence of deoxyribose sugar radicals (*8, 9* and references therein). A few years later, Wang and coworkers suggested the possible existence of sugar radicals in γ-irradiated hydrated DNA at elevated radiation doses (*5*). More recently, increasing evidence for these radicals has been uncovered. Using ESR spectroscopy at 77 K, the C1′ and, possibly, the C4′ or C5′ sugar radicals were reported in γ-irradiated hydrated DNA (*6*). The first clear ESR spectrum of the C1′• in a DNA double helix was reported by Razskazovskii *et al.* (*10*); in this work, C1′• was formed by attack of a radiation-produced hydrogen abstracting agent. A nicely isolated spectra for C1′• in double-stranded DNA at 77 K results from photoexcitation of previously stabilized guanine cation radicals, $G^{+\bullet}$ (*11*). A tentative identification of the C3′• (or C4′•) at 77 K in oxygen-16 ion-irradiated hydrated DNA was made by Becker *et al.* (*12*). The C3′• was also reported in DNA by Weiland and Hüttermann (*13*) after X irradiation and ion-beam irradiation. Very recently, C3′• was reported to be 4.5% of the total radical population in a duplex oligonucleotide [d(CTCTCGAGAG)] X-irradiated and studied at 4 K (*14*). The ESR spectra for the putative C3′• presented previously (*13, 15*) are similar to each other but differ from that reported for d(CTCTCGAGAG); the reason for this difference is yet to be determined. Two other sugar-phosphate backbone radicals have been identified through ESR spectroscopy. A phosphate radical of the type $ROPO_2^{-\bullet}$ has been clearly identified in oxygen-ion-irradiated (*12*), argon-ion-irradiated (*15*), and γ-irradiated (*15*) DNA. This radical originates with P–O bond cleavage, likely through dissociative electron attachment. A complementary sugar moiety radical resulting from rupture of the C3′–O bond was also reported in argon-ion-irradiated and γ-irradiated hydrated DNA (*15*). Both these radicals are important because each is the direct product of a strand break.

[1] Current address: Plant Molecular Biology, International Centre for Plant Genome Research, New Delhi-110067, India.

[2] Address for correspondence: Department of Chemistry, Oakland University, 2200 N. Squirrel Rd., Rochester, MI 48309; e-mail: sevilla@ouchem.chem.oakland.edu.

There are a number of mechanisms through which sugar radicals can be formed through direct-type effects on hydrated DNA samples. In γ-irradiated hydrated DNA samples, more than 50% of the ionizations occur on the sugar-phosphate backbone (direct effect) and adjacent waters of solvation. The first hydration layer rapidly transfers holes to the sugar-phosphate backbone (quasi-direct effect). Because the cation radical thereby formed on the sugar moiety is expected to have a very low pKa, deprotonation of the sugar radical cation is considered to be a principal mechanism by which neutral sugar radicals are formed (*6, 11, 16, 17*). Other mechanisms and possibilities do exist. For example, as just noted, radicals reported from ESR studies support dissociative electron attachment as a likely path for formation of $C3'^{\bullet}_{dephos}$. Furthermore, it has been clearly shown that visible light excitation of the guanine cation radical in DNA results in formation of the C1′ sugar radical (*11*). In model compounds such as nucleotides and nucleosides, it has been shown that hydrogen atoms abstract hydrogen from the sugar moiety to form neutral sugar radicals (*18*). Thus it is conceivable that excited states of neutral bases or sugar moieties in DNA could undergo homolytic bond cleavage to result in hydrogen atoms and, by their reaction, sugar radicals. In addition, if this process were to occur in the sugar group, a neutral sugar radical would directly form. However, there is no evidence, as yet, for either of these processes in hydrated DNA exposed to low-LET radiation at 77 K. Thus, in this work, we assume that deprotonation of sugar cation radicals is the dominant mechanism by which sugar radicals form under the conditions employed.

Methods other than ESR spectroscopy have been used to explore the connection between sugar radicals and strand breaks. An analysis of base damage and undamaged base release in room-temperature γ-irradiated hydrated DNA concluded that about 35% of total ionizations result in sugar radicals and subsequent base release (*17*). Since each ionization also forms an electron that adds to the DNA bases, these results suggest that about 17% of all radicals at low temperatures should be sugar radicals, which is close to the estimates from recent ESR work. A recent report on oligonucleotides examines the relationship between the yields of base release and those of free radical formation and concludes that the yields of released bases are 10–20% of the total free radicals trapped in crystalline oligonucleotides at 4 K (*19*). An extensive literature exists regarding the primary indirect effect, the attack of hydroxyl radicals and hydrated electrons on DNA and the sugar moiety in DNA (*2, 4, 20, 21*). However, this current work is concerned primarily with direct-type effects.

A variety of experimental techniques have been used to obtain the ESR spectra of sugar moiety radicals, which, as stated earlier, normally constitute a small fraction of the radical cohort formed in γ-irradiated DNA. Because they are neutral in charge, they are more resistant to destruction by radiation than are ion radicals (*5, 12, 15*). Thus high doses tend to result in a larger fraction of neutral radicals relative to ion radicals (*5, 6, 15*); in DNA, it appears that most of the initially formed neutral radicals are sugar moiety radicals; thus high doses will emphasize the sugar radicals. It has also been observed that high-LET radiation produces larger fractions of neutral radicals than low-LET radiation (*12, 13, 15*); thus ion-beam irradiation can be used to advantage to investigate the presence and properties of DNA sugar radicals. Last, in an elegant experiment, the electron scavenger $K_3Fe(CN)_6$ was used to greatly reduce the concentration of anion radicals stabilized at 77 K in irradiated DNA and thereby focus on the oxidative path (*6*). Since most of the sugar moiety radicals stabilized at 77 K appear to result from deprotonation of cation radicals, this increased the relative concentration of these radicals and permitted qualitative computer isolation of their ESR spectra (*6*). In this work, we expand on that technique by adding both an electron scavenger and a hole scavenger to DNA samples to better investigate the sugar moiety radicals in irradiated, hydrated DNA at 77 K. This work is directed toward a better understanding of the chemical nature and the distribution of sugar radicals formed by radiation-induced damage to DNA.

MATERIALS AND METHODS

Preparation of DNA Solution

Salmon testes DNA (sodium salt, 57.3% AT and 42.7% GC) was obtained from Sigma Chemical Company and used without further purification. Potassium ferrocyanide, $K_4Fe(CN)_6$, potassium ferricyanide, $K_3Fe(CN)_6$, and D_2O (99.9%) were obtained from Aldrich Chemical Company. DNA solutions, at concentrations of up to 150 mg/ml, were prepared in D_2O that had been flushed with N_2. These solutions were allowed to stand overnight at 4°C to form a homogeneous solution. Scavenger solutions [$K_4Fe(CN)_6$ or $K_3Fe(CN)_6$ or both] were prepared in D_2O at the concentrations required to prepare the desired scavenger/nucleotide ratio. Approximately 1 ml of the DNA solution and an equal volume of the scavenger solution were mixed to prepare complexes in which one scavenger ion per 10 bp was present. Thus samples contained one $K_4Fe(CN)_6$ per 10 bp, or one $K_3Fe(CN)_6$ per 10 bp, or, in samples in which both scavengers were present, one $K_4Fe(CN)_6$ per 20 bp and one $K_3Fe(CN)_6$ per 20 bp. A study of samples in increasing scavenger:base-pair ratios from 1/200 bp to 1/10 bp showed that scavenging was virtually complete at 1/20 bp. Higher scavenging ratios did not increase the amount of scavenging, probably as a result of uneven distribution of the scavenger.

Preparation of DNA ''Ice'' Samples

DNA ''ice'' samples were prepared using the method described earlier (*22*). Aqueous solutions, flushed with N_2, of DNA and DNA with the desired scavengers were drawn into a glass tube with an inner diameter of 4 mm and frozen in liquid nitrogen. The outside of the glass was then quickly warmed just enough to allow the resultant ice plug to be pushed out into liquid nitrogen. The samples were prepared in a nitrogen atmosphere in a glove bag.

Preparation of Hydrated DNA Samples

DNA and DNA/scavenger frozen solutions in D_2O were vacuum-dried to remove water. These samples were then equilibrated over a saturated

KCl/D_2O solution for 6 days under a nitrogen atmosphere. The hydrated samples were then pressed into cylinders (0.4 cm × 1 cm height) under a nitrogen atmosphere using an aluminum dye and press and immediately placed in liquid nitrogen.

Irradiation

Samples were γ-irradiated with ^{60}Co γ rays with a dose of 1 to 160 kGy at 77 K; the dose rate was about 1.5 kGy/h. DNA ice samples were annealed at 130 K for 10 min to remove the ESR signal from hydroxyl (OH) radicals in the crystalline ice phase. This annealing results in a slightly larger yield of neutral radicals (*vide infra*) than that found in comparable γ-irradiated hydrated DNA samples (with and without scavengers) that do not contain significant amounts of ·OH and that were therefore not annealed.

Electron Spin Resonance

All ESR spectra were recorded at 77 K using 6.3 μW power. Spectra were digitalized and stored in computer memory. A Varian Century ESR spectrometer operating at 9.2 GHz with an E-4531 dual-cavity, 9-inch magnet, and low-temperature assembly was employed. Fremy's salt (g = 2.0056 A_N = 1.309 mT) was used for field calibration; the position of the three Fremy salt resonances are indicated on the ESR spectra shown. All spectra were recorded within a few minutes of irradiation.

Computer Analysis

The methods of computer analysis were similar to those described in our previous work (*22*). Linear least-squares fittings of benchmark spectra were employed to determine the fractional composition of radicals in experimental spectra. Computer analyses were done with ESRADSUB and ESRPLAY (both developed in our laboratory). The origin of the benchmark spectra used is given in the Appendix.

Since a focus of this work is the fate of electron-gain and electron-loss radicals, we have not presented separate analyses of the amounts of $T^{\cdot-}$ and $C(N3)H^{\cdot}$ as was done in earlier work (*5*). Thus these electron-gain radicals are denoted together by the symbol $DNA^{\cdot-}$. The principal electron-loss radical stabilized at 77 K is $G^{\cdot+}$ and is indicated as such. The complex mixture of neutral radicals formed is denoted by the symbol $\Sigma N_i^{\cdot}$; its actual composition, and therefore the form of its ESR spectra, may depend on the conditions under which the mix of radicals is formed and the manner in which the composite spectrum is derived. For this work, the composite ESR spectrum derived for $\Sigma N_i^{\cdot}$ did not change significantly with dose, and no change was detected in $\Sigma N_i^{\cdot}$ with different loadings of scavenger, although some subtle changes might well be expected.

Calculation of G Values (Yields)

Except where noted, G and k values were obtained from a least-squares fit of data to Eq. (1),

$$C = C_{max}(1 - e^{-kD}), \quad (1)$$

in which C is the radical concentration (μmol/kg) at dose D (Gy), C_{max} (= G/k) the maximum radical concentration at dose saturation, G the radical yield at low dose (μmol/J), and k the radiation destruction constant (Gy^{-1}). To determine G and k values, all data points up to 200 kGy were fitted to the indicated equation.

In two samples (*vide infra*) in which a decrease in radical concentration with increasing dose was observed, Eq. (1) is unable to properly represent the dose response. Thus Eq. (2), which includes a term to describe such a decrease, is used instead (*5*).

$$C = (G/k - k'/k^2)(1 - e^{-kD}) + k'D/k. \quad (2)$$

The constant k' originates with a term ($-k'D$) in the differential equation that describes the change in concentration with dose. The specific meaning of k depends on the mechanism by which the decrease in radical occurs. Equation (2) predicts that if k' is positive, the concentration of radicals will increase without limit with increasing dose; nonetheless, in the limited dose ranges used in our laboratory, Eq. (2) has been very successful in describing the observed dose–response data.

Terminology

In DNA, the pertinent known *charged* radicals are the pyrimidine anion radicals, i.e. the thymine anion radical ($T^{\cdot-}$) and the reversibly protonated cytosine anion radical [$C(N3)H^{\cdot}$], and the guanine cation radical ($G^{\cdot+}$). Even though $C(N3)H^{\cdot}$ is protonated from its base pair G, the CG base pair itself remains an anion radical and is experimentally found to behave as part of the charged cohort (*21*). Also, $G^{\cdot+}$ in double-stranded DNA may partially deprotonate to its base pair C, but again the base pair remains a cation radical (*21*). Because of coulombic attractions, charged radicals are more susceptible to recombination from holes and electrons produced by radiation than are neutral radicals. Thus we use the term ''neutral radicals'' to connote a cohort of radicals that are resistant to radiation destruction. As indicated earlier, the concentration of neutral radical(s) does not readily reach a plateau at high dose, and therefore, at high dose, the concentration of neutral radicals increases with dose faster than the concentration of charged species. As expected, charged radicals are also far more susceptible to undergoing a reaction with one-electron redox agents than are neutral radicals (*vide infra*).

The details of the structure of the ESR spectrum attributed to a ''neutral radical'' cohort will depend on experimental conditions, such as the redox agents employed; however, our current working hypothesis, which is explored in this work, is that the neutral radical cohort is made up predominantly of deoxyribose sugar radicals. In this regard, it is possible that small amounts of neutral base radicals are present in the neutral radical cohort we observe. With the techniques available, we have not found clear evidence for this at this time.

For readability, DNA samples containing the hole scavenger $Fe(CN)_6^{4-}$ are often denoted as ''Fe^{2+}/DNA'' samples and those containing the electron scavenger $Fe(CN)_6^{3-}$ are given the symbol ''Fe^{3+}/DNA.''

RESULTS

γ-Irradiated DNA in Presence of Electron and Hole Scavengers

Figure 2A–D shows the ESR spectra of ice plugs of DNA (75 mg/ml D_2O) obtained at 77 K after γ irradiation with a dose of 27 kGy at 77 K and annealing to 130 K. The spectrum in Fig. 2A results from a sample with no scavengers present and is indistinguishable from spectra published earlier for D_2O hydrated DNA samples (*9*, *11*, *21*). The spectrum in Fig. 2B originates with DNA in which $Fe(CN)_6^{4-}$, a hole scavenger, has been added at a ratio of one $Fe(CN)_6^{4-}$ per 10 bp. As expected, this sample contains a considerably lower percentage of guanine cation radicals than DNA without scavenger (Table 2), and the broad centrally located singlet from $G^{\cdot+}$ (Fig. 1A) is largely missing. The remaining doublet spectrum in Fig. 2B results predominantly from DNA anion radicals and neutral radicals. The spectrum in Fig. 2C originates with DNA in which $Fe(CN)_6^{3-}$, an electron scavenger, has been added at a ratio of one $Fe(CN)_6^{3-}$ per 10 bp. As expected, this sample contains a considerably lower percentage of pyrimidine one-electron-reduced radicals than DNA without scavenger (Table 2). The loss of the pyrimidine one-electron-reduced radicals is seen in the diminution of the centrally located about

TABLE 1
Structure of Radicals

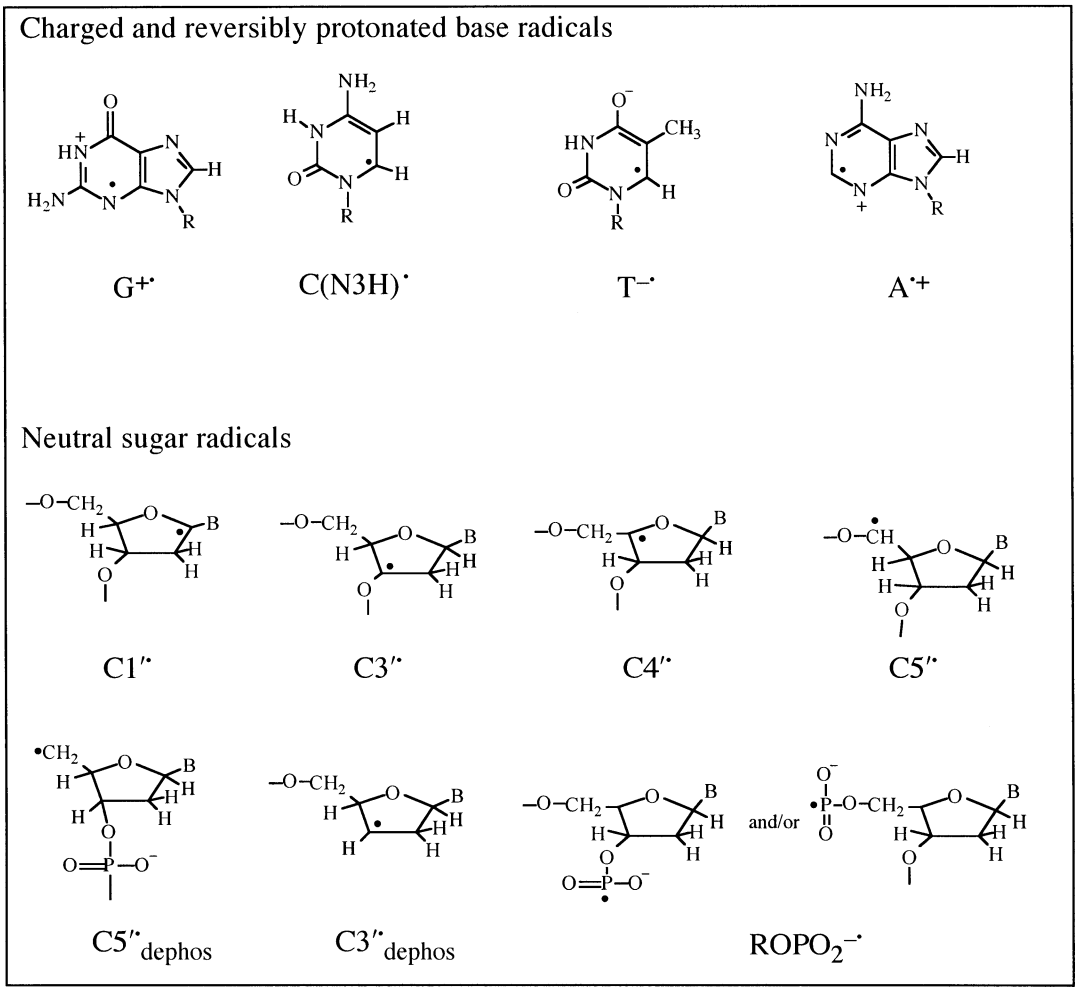

1.6–1.8 mT doublet(s) (Fig. 1B and C) from the DNA spectrum. We attribute the spectrum that remains predominantly to guanine cation radicals and neutral radicals. Figure 2D is the spectrum of a DNA sample in which both the hole scavenger $Fe(CN)_6^{4-}$ and the electron scavenger $Fe(CN)_6^{3-}$ have been added, each at a 1:20 scavenger:bp ratio. Our analysis indicates that the spectrum originates principally with the neutral radical cohort and a small amount of C(N3)H• (Table 2). As can be seen from Table 2, the neutral radical cohort is present in all of the spectra shown in Fig. 2.

The approximately 2.0 mT central doublet splitting in Fig. 2D is similar to but slightly larger than the approximately 1.6–1.8 mT found for the pyrimidine anion radicals in the spectra shown in Fig. 1B and C; this creates some difficulty in determining its assignment. However, the species causing the remaining doublet is clearly not scavengeable, even at high loadings of scavenger, nor does it undergo radiation destruction as the DNA anion radicals do; thus it can be differentiated from the doublet(s) from the DNA anion radicals, C(N3)H• and $T^{\bullet-}$. The inability to scavenge the radical responsible for this doublet (Fig. 2D) and its resistance to radiation destruction lead to the hypothesis that it arises from a neutral radical.

Similar results are observed in hydrated ($\Gamma = 14 \pm 2$ D_2O/nucleotide) DNA. Figure 3 presents the ESR spectra of γ-irradiated hydrated DNA samples. Because no hydroxyl radical is formed in these samples, they were not annealed at 130 K as were the samples in ice. The spectrum in Fig. 3A for a sample with no scavengers present is indistinguishable from that presented earlier (*22*). Addition of the hole scavenger $Fe(CN)_6^{4-}$ results in substantial loss of the centrally located singlet from $G^{\bullet+}$ (Fig. 1A) as shown by the improved resolution of the $DNA^{\bullet-}$ doublet in the center of the spectrum (Fig. 3B). With the electron scavenger $Fe(CN)_6^{3-}$ present, the doublet(s) from $DNA^{\bullet-}$ (Fig. 1B and C) largely disappears (Fig. 3C). With both $Fe(CN)_6^{4-}$ and $Fe(CN)_6^{3-}$ present, both $G^{\bullet+}$ and $DNA^{\bullet-}$ are largely scavenged, and the spectrum that remains is attributed largely to a mixture of neutral radicals.

The wings of these spectra indicate that a spectrum from the neutral radical cohort is present in all of the spectra

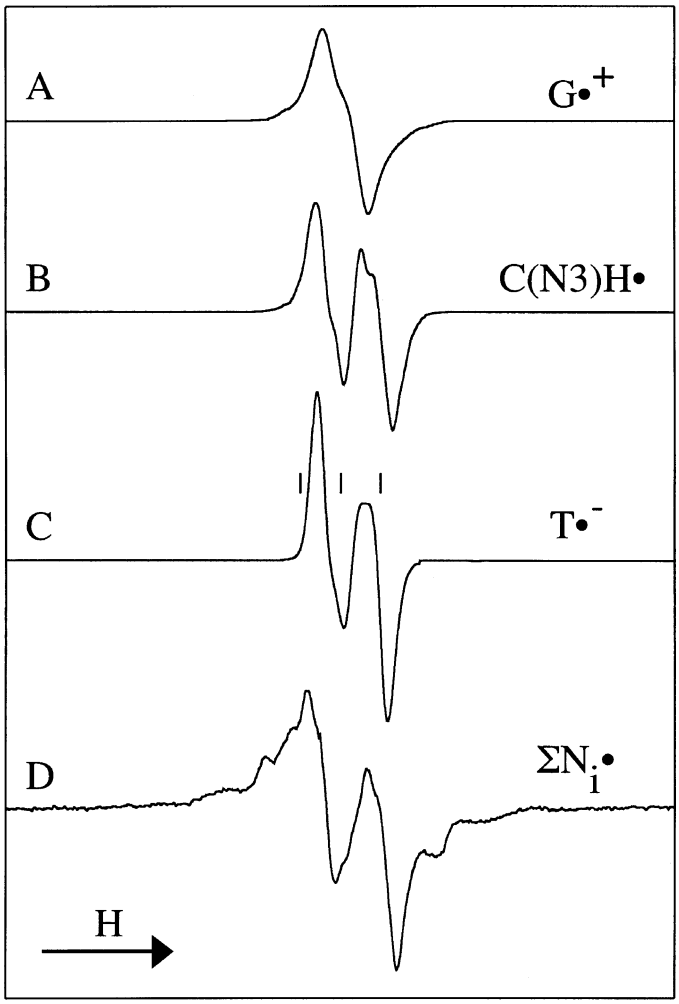

FIG. 1. ESR benchmark spectra used for analysis of spectra and data in Figs. 2–6. The origin of these is described in the Appendix. A: Guanine cation radical ($G^{\bullet+}$). This radical is likely deprotonated in part from N1. B: Cytosine anion radical, reversibly protonated at N3. C: Thymine anion radical. D: Mixture of neutral radicals, $\Sigma N^{\bullet}$, thought to be mostly sugar radicals. The three hatch marks/small spectra in this and other figures indicate the Fremy salt resonances with $g = 2.0056$ and $A_N = 13.09$ G.

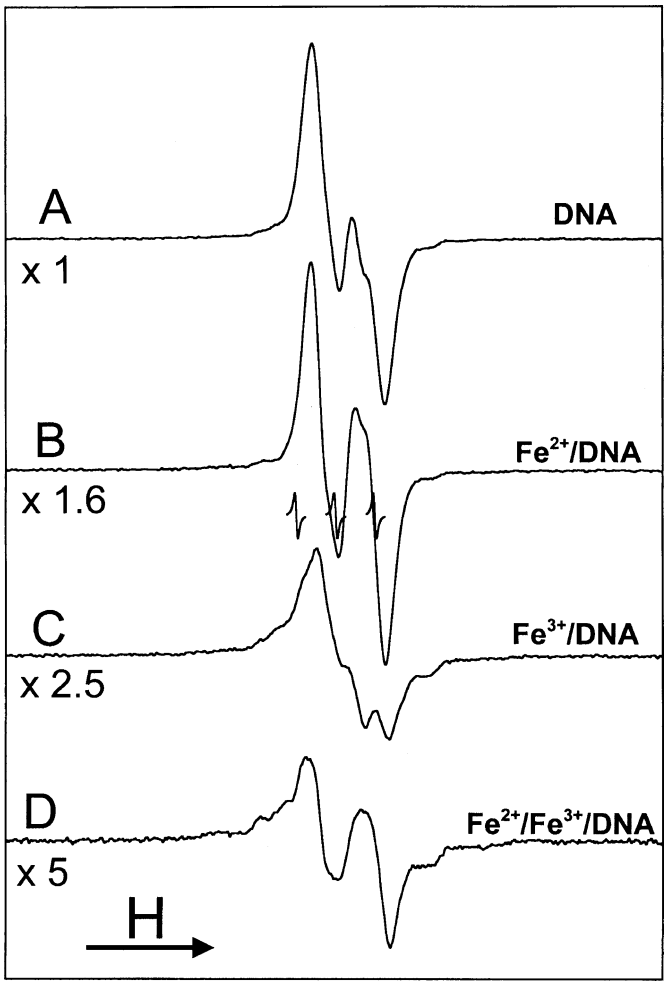

FIG. 2. ESR spectra of frozen ice DNA samples (75 mg/ml) γ-irradiated with a dose of 27 kGy. The samples were annealed to 130 K for 10 min to remove the hydroxyl radical signal before recording the spectrum at 77 K. The relative spectrometer gain used for each sample is indicated. A: DNA with no scavengers present. B: DNA with one $Fe(CN)_6^{4-}$ per 10 bp. C: DNA with one $Fe(CN)_6^{3-}$ per 10 bp. D: DNA with one $Fe(CN)_6^{4-}$ per 20 bp and one $Fe(CN)_6^{3-}$ per 20 bp.

shown in Fig. 3. The amplified wing spectra were recorded at a higher doses and at higher spectrometer gain than the central spectra. As can be seen, the shape of the outer components does not depend on the scavengers present.

Dose–response curves for two sets of hydrated DNA samples are shown in Fig. 4; these are representative of the dose responses found. For these and other analyses, the benchmark spectra shown in Fig. 1 were used to determine the composition of each composite spectrum at each dose and the dose response of each component analyzed. Equation (1) was used to obtain all the fits (solid lines) shown in the figure, except for $G^{\bullet+}$ in the Fe^{3+}/DNA sample (Fig. 4B), for which Eq. (2) was used.

The *G* values obtained in these analyses are shown in Fig. 5 and Table 3. For DNA without scavenger present, the values obtained were well within experimental error of those obtained in a very extensive earlier investigation (*5*, *22*). Thus we consider these *G* values to be good estimates, especially for relative yields between samples with differing scavengers.

As expected, addition of the hole scavenger $Fe(CN)_6^{4-}$ (''Fe^{2+}/DNA'') results in a large decrease in the yield of $G^{\bullet+}$ stabilized at 77 K. The yield of reductive path radicals

TABLE 2
Analysis of Radical Composition for Spectra Shown in Fig. 2

	Percentage[a]			
Sample	$G^{\bullet+}$	C(N3)H•	$T^{\bullet-}$	$\Sigma N_i^{\bullet}$
DNA	40	38	10	12
DNA/Fe^{2+}	12	45	18	26
DNA/Fe^{3+}	43	9	0	48
DNA/Fe^{3+}/Fe^{2+}	0	19	0	81

[a] Estimated relative error is ±20%.

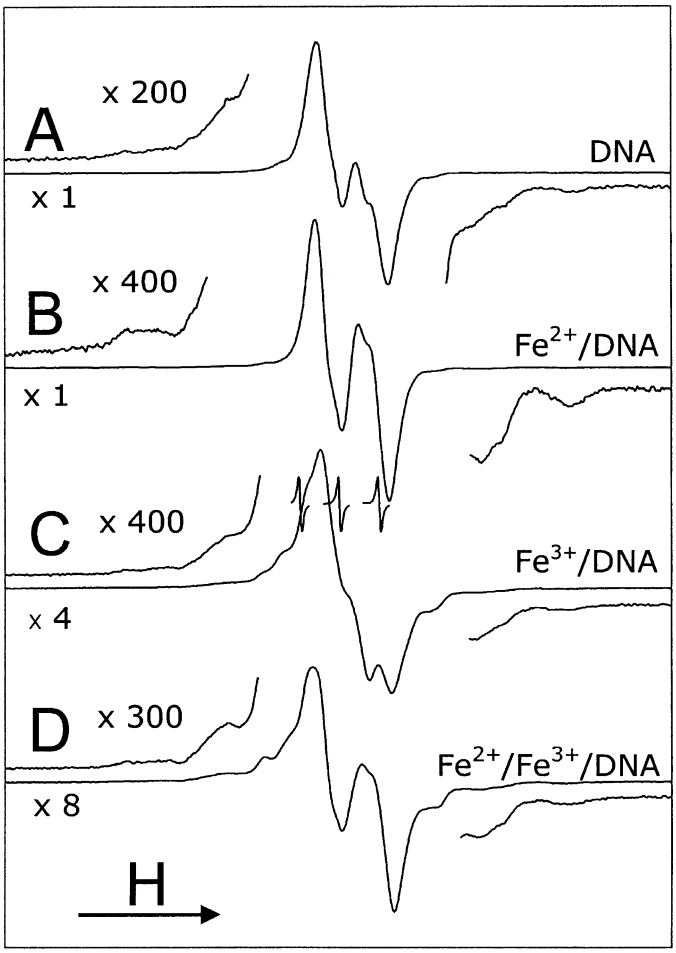

FIG. 3. ESR spectra at 77 K of γ-irradiated hydrated ($\Gamma = 14 \pm 2$) DNA samples. A: DNA with no scavengers present. B: DNA with one $Fe(CN)_6^{4-}$ per 10 bp. C. DNA with one $Fe(CN)_6^{3-}$ per 10 bp. D: DNA with one $Fe(CN)_6^{4-}$ per 20 bp and one $Fe(CN)_6^{3-}$ per 20 bp. The spectrum in A is from a sample γ-irradiated with a dose of 7 kGy; the spectra with C–D are from samples γ-irradiated with a dose of 12 kGy. The amplified wing spectra in A–D are from the same samples, γ-irradiated with a dose of 38 kGy. The gain for each spectrum relative to the x1 for the unamplified spectra in A and B is indicated on each.

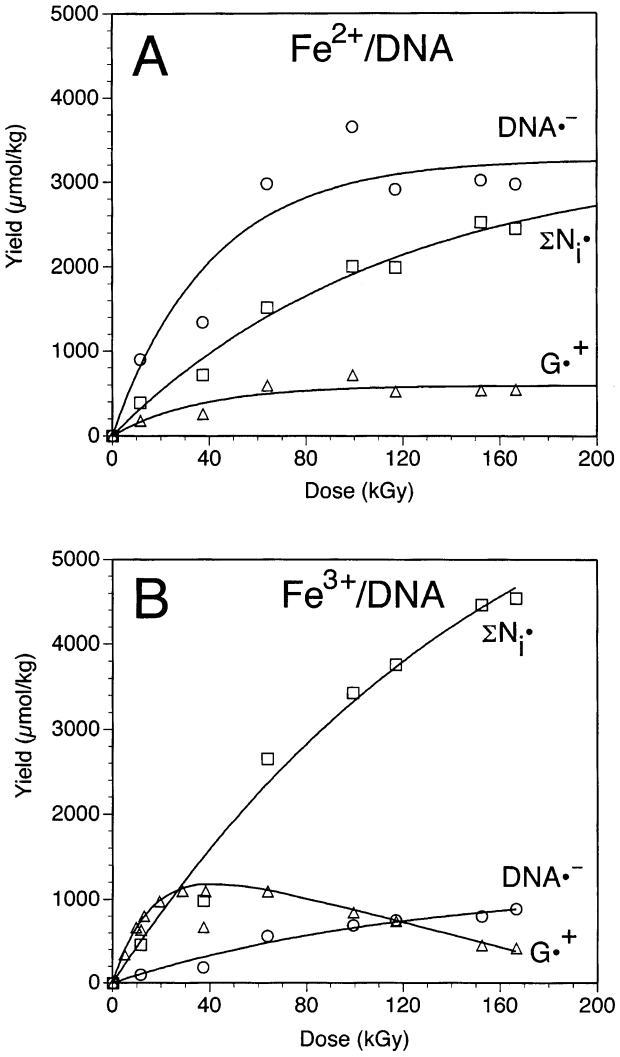

FIG. 4. Representative dose–response curves for two of the four types of hydrated DNA samples investigated. Analyses were completed using the benchmark spectra in Fig. 1; the yield for $DNA^{\bullet -}$ is the sum of the yields of $C(N3)H^{\bullet}$ and $T^{\bullet -}$. Panel A: Dose response for radicals in samples with one $Fe(CN)_6^{4-}$ per 10 bp. The curve shown results from the fit of each set of data to Eq. (1). B. Dose response of radicals in samples with one $Fe(CN)_6^{3-}$ per 10 base pairs. The curve shown results from the fit of each set of data to Eq. (1) (for $\Sigma N^{\bullet}$ and $DNA^{\bullet -}$) or Eq. (2) (for $G^{\bullet +}$). The *G* value in Table 3 for each radical is given by these fits.

[$DNA^{\bullet -}$] is only slightly less than that found with no scavenger present. The slight decrease in neutral radical yield is reproducible and suggests that $Fe(CN)_6^{4-}$ scavenges only small amounts of the neutral radicals or their putative cationic precursors. With the electron scavenger $Fe(CN)_6^{3-}$ present (''Fe^{3+}/DNA''), a significant decrease in the yield of the reductive path radicals occurs, as expected. There is also a decrease in formation of $G^{\bullet +}$; we attribute this to formation of $Fe(CN)_6^{4-}$ as $Fe(CN)_6^{3-}$ scavenges electrons, and scavenging of $G^{\bullet +}$ (or precursor holes) by the $Fe(CN)_6^{4-}$ thus formed. A substantial and reproducible increase in the yield of neutral radicals is observed and likely results from the fact that the capture of electrons (free or from anion radicals) by $Fe(CN)_6^{3-}$ prevents their recombination with the neutral radicals or their precursor cation radicals (see Discussion). With both $Fe(CN)_6^{3-}$ and $Fe(CN)_6^{4-}$ present, the yields of $G^{\bullet +}$ and $DNA^{\bullet -}$ are quite small, and the spectra obtained are attributed almost entirely to neutral radicals. The yield of neutral radicals is about the same as that found with only $Fe(CN)_6^{3-}$ present. This is further evidence that $Fe(CN)_6^{4-}$ is not effective in scavenging the holes or cation precursors to the neutral radical cohort and that the scavenging of electrons and/or anion radicals results in larger yields of neutral radicals than would otherwise occur.

Figure 6 shows the fraction of each type of radical present as a function of dose. In viewing Fig. 6 it should be remembered that the absolute yield of each radical generally (but not in every case) increases (or increases to a plateau) with increasing dose.

In Fig. 6A, the fractions of each type of radical found in

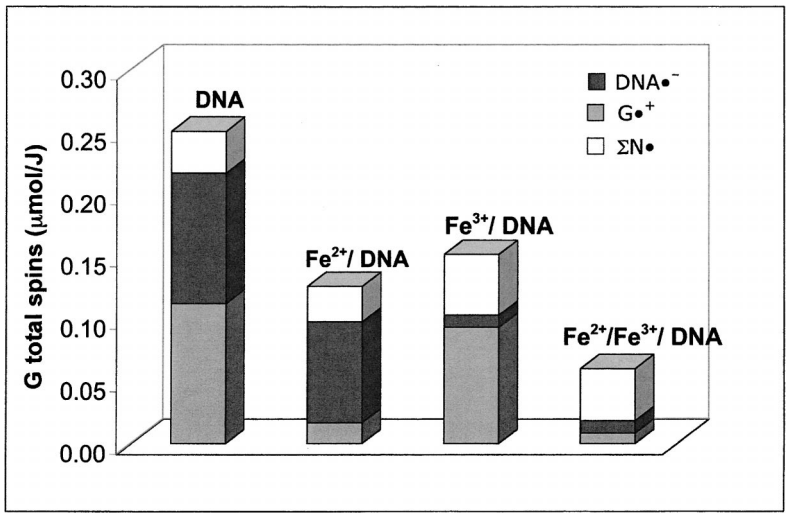

FIG. 5. Bar graph of *G* values of hydrated ($\Gamma = 14 \pm 2$) DNA samples with and without scavengers. *G* values were obtained from dose–response curves like those shown in Fig. 4; the scavenger ratios used are the same as those cited in Fig. 4. This figure is a graphic representation of the values shown in Table 3.

γ-irradiated hydrated DNA with no scavenger present are shown. The results are similar to earlier analyses of irradiated DNA (*5, 9*) except that we are now better able to characterize the fraction of neutral radicals present. With the model that a *large majority* of the neutral radicals originates with the electron-loss path, the zero-dose extrapolation is reasonably close to the 50:50 ratio expected between electron-loss and electron-gain radicals and within the errors inherent in these analyses. With increasing dose, the percentages of the radiation-resistant neutral radicals increase as those of the more radiation-sensitive charged radicals decrease.

Figure 6B shows the results obtained when the hole scavenger $Fe(CN)_6^{4-}$ is added to an identically handled sample. As expected, the initial percentage of $G^{+\cdot}$ (12% at the zero-dose extrapolation) is far lower than that in samples with no scavenger present. With increasing dose, the percentage of radiosensitive $G^{+\cdot}$ and of $DNA^{\cdot -}$ each falls slightly, whereas that of the radioresistant neutral radicals increases.

In Fig. 6C, which gives results for samples with the electron scavenger $Fe(CN)_6^{3-}$ present, there is very efficient suppression of the electron-gain path at all doses. With increasing dose, a point is reached in which the neutral radical component appears to reach a plateau at about 82% of the radicals and $G^{+\cdot}$ at about 8%. The decreasing percentage of $G^{+\cdot}$ likely results from scavenging of $G^{+\cdot}$ and/or its precursors by $Fe(CN)_6^{4-}$ formed as $Fe(CN)_6^{3-}$ scavenges electrons.

In Fig. 6D, we display the results observed for DNA samples with both the hole scavenger $Fe(CN)_6^{4-}$ and electron scavenger $Fe(CN)_6^{3-}$ present. At high dose, the percentage of $G^{+\cdot}$ trends to zero and that of the neutral radicals increases to about 90%; again, the actual yield of $G^{+\cdot}$ decreases with increasing dose (not shown). It is possible that the formation of additional (hole scavenger) $Fe(CN)_6^{4-}$ beyond that originally present, as $Fe(CN)_6^{3-}$ scavenges electrons, causes an actual decrease in the concentration of $G^{+\cdot}$. A most important aspect of this particular experiment is that, at high doses, the ESR spectrum obtained originates almost entirely with neutral radicals.

TABLE 3
***G* Values for Hydrated DNA Samples**

	G(μmol/J)[a]			
	DNA	Fe^{2+}/DNA	Fe^{3+}/DNA	Fe^{2+}/Fe^{3+}/DNA
DNA^-	0.11	0.081	0.010	0.008
$G^{+\cdot}$	0.11	0.017	0.093	0.010
$\Sigma N^{\cdot}$	0.034	0.029	0.049	0.042
Sum	0.25	0.13	0.15	0.060

[a] Estimated relative error is ±20%.

DISCUSSION

The Sugar Radicals

A principal purpose of this work is to gain insight into the ESR spectral parameters and the concentrations of the deoxyribose sugar radicals found in γ-irradiated DNA. As stated earlier, our current working hypothesis is that the neutral radical cohort which gives rise to the largest components of the spectra shown in Figs. 1D, 2D and 3D is made up principally of these deoxyribose radicals. In addition, we have concluded previously that deoxyribose radicals from the direct effect result principally from deprotonation of sugar cation radicals (*15*); $C3'^{\cdot}_{dephos}$, which has been attributed to dissociative electron attachment (*12, 15*), is the only previously known exception to this conclusion for hydrated DNA irradiated at 77 K with low-LET radiation.

As a first step in understanding the makeup of the neutral radical cohort, in Fig. 7 we compare discernible spectral

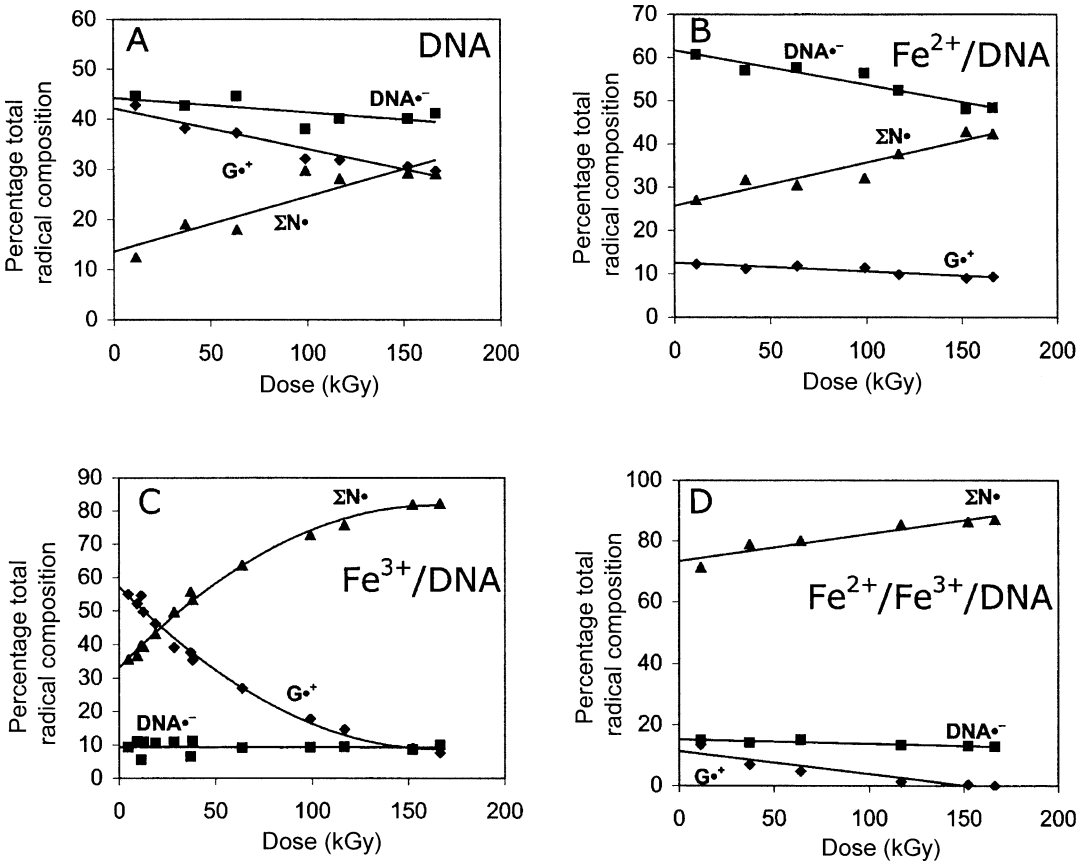

FIG. 6. Percentages of each type of radical present in hydrated ($\Gamma = 14 \pm 2$) DNA samples with and without scavengers present. The scavenger ratios are the same as those cited in Fig. 4. Analyses were done on unannealed samples for which the spectra were recorded at 77 K, using the benchmark spectra from Fig. 1.

components from a neutral radical cohort ESR spectrum with a variety of experimental or simulated spectra of deoxyribose sugar radicals. The spectrum in Fig. 7A is from a hydrated DNA sample irradiated with a relatively high dose (152 kGy) with both $Fe(CN)_6^{3-}$ and $Fe(CN)_6^{4-}$ present each at a 1:20 scavenger:base-pair ratio. An analysis of the experimental spectrum, using the neutral radical benchmark spectrum from Fig. 1D and the C(N3)H· spectrum from Fig. 1B, indicates it is composed of about 87% of the spectrum of $\Sigma N_i^{\cdot}$ and 13% of that from C(N3)H·. Amplified wing scans show the presence of spectral components that are not present in the DNA base spectra from Fig. 1A–C. In Fig. 7B, the spectra shown are those of Fig. 7A from which the spectrum for C(N3)H· has been subtracted as 13% of the integrated intensity. The neutral radical cohort spectrum that results is similar to that shown in Fig. 1D (from a lower-dose spectrum) and compares favorably to the neutral radical cohort spectra derived from DNA samples irradiated with a high-LET argon-ion beam (*15*). The amplified wing component spectrum in Fig. 7B is identical to that in Fig. 7A because the C(N3)H· spectrum has zero intensity in the amplified wing region.

In Fig. 7C–G are shown the spectra of likely neutral radicals that contribute to the composite spectrum in Fig. 7B; their origins are described in the Appendix. Qualitatively, the outer line components of the $C3^{\cdot}_{dephos}$, C3′· and C1′· are visible in the spectra shown in Fig. 7B. The visible line components from $C3^{\cdot}_{dephos}$ are denoted by asterisks (*); the four proton hyperfine couplings present in this radical place the outer line components 13.4 mT apart and clearly are visible in the expanded wings of the composite neutral radical spectrum. The outer line components of C3′·, 7.7 mT apart (denoted by daggers, †), are also visible in the wings of both the amplified and unamplified spectra in Fig. 7B. Although these line components overlap inner components from $C3^{\cdot}_{dephos}$, the intensity present in the composite spectrum appears too large to be attributed to $C3^{\cdot}_{dephos}$ alone. Narrower line components consistent with the outer components of C1′· are also present in the composite spectrum in panel 7B (arrows, ↓); these are 5.2 mT apart.

The centrally located approximately 2.1 mT doublet in Fig. 7B remains unassigned. Since the radical causing this feature is not easily scavengeable and does not readily dose saturate, we believe it is a neutral radical. Close has speculated that both the C4′· and C5′· in DNA may give rise to an ESR doublet (*27*); however, the coupling in these radicals is very sensitive to the radical(s) environment and conformation, so it is not possible to definitively conclude that

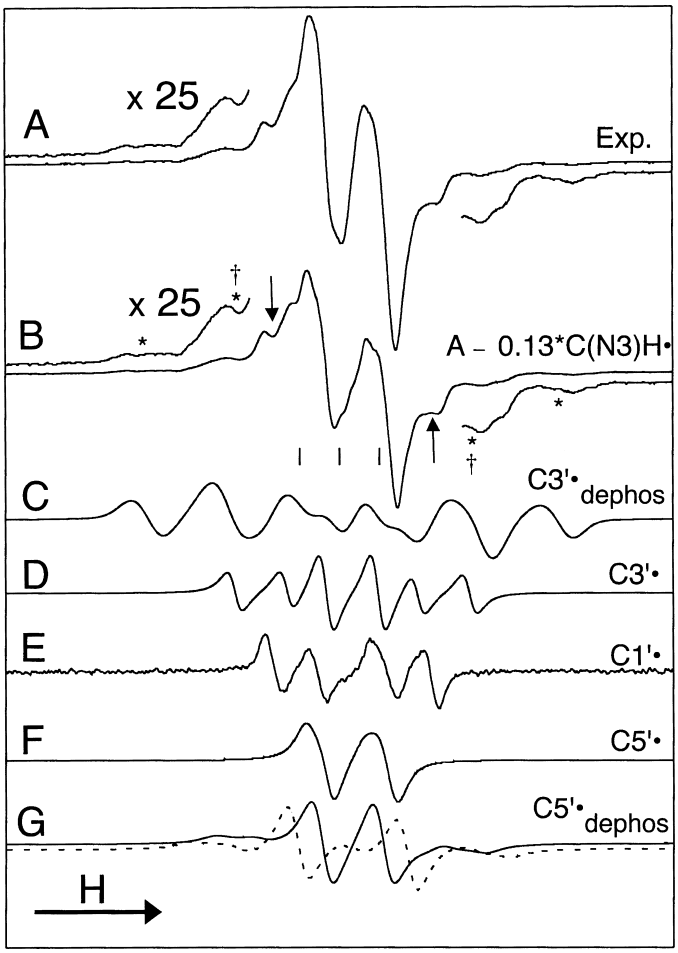

FIG. 7. ESR spectra of hydrated ($\Gamma = 14 \pm 2$) DNA sample and putative spectra of various deoxyribose sugar radicals. A: Experimental spectrum from DNA sample containing both $Fe(CN)_6^{3-}$ and $Fe(CN)_6^{4-}$ at the ratios cited in Fig. 4 and irradiated with a dose of 152 kGy. Analysis of this spectrum using the benchmark spectra from Fig. 1 indicated that it is a composite of 87% ΣN• and 13% C(N3)H•. The amplified wing spectrum is from the same sample, irradiated with a total dose of 169 kGy, and recorded at 25 times the spectrometer gain of the unamplified spectrum. B: Spectra resulting from subtracting the spectrum of C(N3)H• (Fig. 1B) as 13% of the total intensity from the spectra in A; the resulting spectra represent a neutral radical cohort only. The significance of the various symbols used in panel B are described in the narrative. C: Simulated ESR spectrum of $C3'^{\bullet}_{dephos}$. D: Simulated ESR spectrum of C3′•. E: Experimental spectrum of C1′• in DNA (*11*). F: Simulated ESR spectrum of a possible C5′•; the C4′• spectrum may give a similar spectrum, as noted. G: Simulated ESR spectra of $C5'^{\bullet}_{dephos}$ using a hyperfine coupling of 3.6 mT for the C4′ hydrogen (dotted line) or a 2.0 mT coupling for the same proton (solid line). The origins of spectra C–G are given in the text and the Appendix.

the doublet in Fig. 7B is from C5′• and/or C4′•. The simulated spectrum shown in Fig. 7F is that from a C5′• with the assumption of a π-spin density of about 0.85 on C5′ and no resolvable β-couplings to the hydrogen atoms on C4′ (*27*). A C4′• with only one β coupling of about 2.2 mT might result in a very similar spectrum. We hasten to point out that there are no experimental reports of the spectra of either the C4′• or C5′• in DNA; the spectrum in Fig. 7F is a conjecture based on the existence of the doublet from an unscavengeable radical in Fig. 7A and the spectra presented in ref. (*27*).

A second possibility that is consistent with the spectrum in Fig. 7B is that the central doublet results in part from the presence of the $C5'^{\bullet}_{dephos}$. A $C5'^{\bullet}_{dephos}$ has been observed at 77 K in a single crystal of deoxycytidine 5′-monophosphate monohydrate (*23*). The hydrogen hyperfine couplings derived were A(2H) = (−1.06, −2.04, −3.45) mT and A(1H) = 3.6 mT. The simulated spectrum for this radical, using these experimental couplings (Fig. 7G, dotted line), does not match line components in the experimental spectrum in Fig. 7B very well. On the other hand, it is well known that β-hydrogen hyperfine couplings are very sensitive to the dihedral angle (θ) between the β-hydrogen C–H bond and the radical site p-orbital axis. A DFT B3LYP optimization was performed on the $C5'^{\bullet}_{dephos}$ model system (Scheme 1) with the 6–31G(d) basis set followed by calculation of radical EPR parameters using the EPR-III basis set. This calculation results in hyperfine couplings [A(1H) ≈ 3.7 mT, A(2H) ≈ (−3.5, −2.2, −1.0) mT] very close to the experimental values just cited; the calculation also gave a dihedral angle of 43°. A calculation performed after rotation of the CH_2 group by 20°, to a dihedral angle of 63°, results in a hyperfine coupling constant of 2.0 mT for the C4′ hydrogen atom. A simulated ESR spectrum using this coupling and the previously cited experimental couplings for the two α protons results in a spectrum (Fig. 7G, solid line) that nicely matches line components in the spectrum in Fig. 7B.

We finally note that high-level theoretical calculations reported for the electron-induced cleavage of the O–C3′ and O–C5′ bonds in a model system indicate that cleavage of each bond is equally probable (*24*). Thus it is expected that roughly equal amounts of $C5'^{\bullet}_{dephos}$ and $C3'^{\bullet}_{dephos}$ should form in irradiated DNA, and therefore $C5'^{\bullet}_{dephos}$ is expected to be part of the neutral radical cohort found. Further work will be needed to quantify this radical's ESR spectrum and its contribution to the neutral radical cohort.

We have estimated the fractional composition of sugar radicals in the neutral radical cohort by subtraction of the benchmark spectra in Fig. 7C–G from the neutral cohort spectrum in Fig. 7B. This resulted in the following estimates for percentages of each benchmark spectrum in the neutral radical cohort: C1′•, 6%; $C3'^{\bullet}_{dephos}$, 8%; C3′•, 4%; $C5'^{\bullet}_{dephos}$ + C5′•, ≤30%. We believe the estimates for C1•, $C3'_{dephos}$ and C3′• are fairly reliable. Because the (very preliminary) benchmark spectra for $C5'^{\bullet}_{dephos}$ and C5′• are both

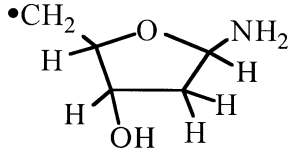

SCHEME 1.

dominated by an approximately 2.0 mT doublet, these two spectra cannot be reliably distinguished from each other in the subtraction process. At this time, we have no firm insight regarding the identity of the remaining radicals (about half of the neutral radical cohort) that cause the composite spectrum that results after the sugar radicals are subtracted out.

We note that the (neutral) radical G(X)• (in which a nonmagnetic moiety X, such as −OH, is bonded to C8 on guanine) can also give rise to a broad central ESR doublet. However, the precursor to G(X)• is $G^{\bullet+}$ itself, a long-lived radical that is readily scavenged by $Fe(CN)_6^{4-}$. In addition, the original spectrum of the sample from which Fig. 7A is derived shows that no observable $G^{\bullet+}$ is present, likely as a result of the scavenging and high dose. These factors all mitigate against the doublet originating with the guanine C8 addition radical.

As indicated earlier, the $C3^{\bullet}_{dephos}$, C3′• and C1′• have been detected in low-temperature irradiated DNA through the use of computer subtraction techniques. We believe this is the first example of the preparation of samples in which these radicals, as well as other possible sugar radicals, have been largely isolated (as a group or radicals) through the use of electron and hole scavengers and the application of high doses.

Scavenging Processes

The electron and hole scavengers employed in this work functioned well. As seen in Figs. 5 and 6, the hole scavenger $Fe(CN)_6^{4-}$ lowered the yield of $G^{\bullet+}$ relative to samples with no scavenger present, and the electron scavenger $Fe(CN)_6^{3-}$ lowered the yield of the electron-gain radicals ($DNA^{\bullet-}$) relative to samples with no scavenger present.

However, there were two unanticipated effects observed with the scavengers. The first is that $Fe(CN)_6^{4-}$ does not cause a significant diminution in the formation of the neutral radical cohort. Since we believe, when dealing with the direct and quasi-direct effect, that the precursors to the neutral radicals are predominantly deoxyribose cation radicals, it appears that $Fe(CN)_6^{4-}$ does not efficiently scavenge short-lived holes. For the cation radical precursor ($DNA^{\bullet+}$), there is a competition between deprotonation to form a neutral radical and hole transfer from the precursor to $Fe(CN)_6^{4-}$ to repair the DNA (Scheme 2). On average, when the scavenger:bp ratio employed is 10:1, any newly formed hole is about 5 bp from a $Fe(CN)_6^{4-}$, a distance of about 1.7 nm. This distance suggests that hole tunneling would occur on a time scale of 1–100 μs, far too slow to compete with deprotonation, which likely occurs in a few vibrations (picoseconds). Thus deprotonation is expected to be the dominant process, as is found.

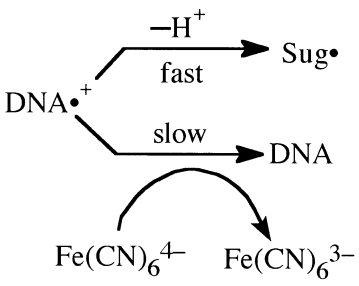

SCHEME 2.

A second interesting and unexpected observation is the decrease in the absolute yield of $G^{\bullet+}$ as a function of dose (Fig. 4B) and the concomitant decrease in its percentage of the radicals observed (Fig. 6C, D) for two samples (hydrated Fe^{3+}/DNA and hydrated Fe^{2+}/Fe^{3+}/DNA); the decrease in absolute yield is far larger than that earlier observed for $G^{\bullet+}$ in scavenger-free samples (*5*) and indicates that most previously stabilized G^+ radicals are destroyed by irradiation. This is likely accomplished by formation of the hole scavenger $Fe(CN)_6^{4-}$ from $Fe(CN)_6^{3-}$ by electron capture. However, the specific mechanism by which a single ionization results in the net destruction of one or more pre-existing G^+ cation radicals is not yet known, and several possibilities exist. For example, it is clear that when $Fe(CN)_6^{3-}$ gains an electron at 77 K, the $Fe(CN)_6^{4-}$ that forms is not in its most stable conformational/solvation state (its surrounding ionic atmosphere, for example, is that of a −3 ion). This likely makes it more reducing than expected and thus would potentiate any mechanism in which $Fe(CN)_6^{4-}$ acts as a reducing agent.

We further note that in all samples, the diminution in the percentage of $G^{\bullet+}$ with increasing dose is larger than that of $DNA^{\bullet-}$ (Fig. 6). We attribute this to the existence of an overall reducing (in the chemical sense) environment in the irradiated samples at 77 K. After early processes (such as geminate recombination) are complete, about 20% of the surviving holes end up as neutral radicals; these radicals are unlikely to act as oxidizing or reducing agents owing to their neutral charge and predicted reduction potentials (*25*). However, electrons cause little neutral radical formation (at 77 K); the excess of surviving electrons over holes results in an overall reducing environment. The loss of $G^{\bullet+}$ in Fe^{2+}/DNA samples (Fig. 4B) and Fe^{2+}/Fe^{3+}/DNA samples (not shown) is likely a result in part of this reducing environment. The positive reduction potential of $Fe(CN)_6^{3-}$ [E_o = +0.36 V] (*26*) would seem to mitigate against this effect because $Fe(CN)_6^{3-}$ is a good oxidizing agent. However, the aforementioned possibility of the buildup of the concentration of a ''high-energy'' form of $Fe(CN)_6^{4-}$ as a result of radiation at 77 K would certainly lower this reduction potential so that a concentration of more effective reducing agents would be produced with radiation.

Further investigation of the scavenging processes and the makeup of the neutral radical cohort is under way in our laboratory.

APPENDIX

Origin of Benchmark Spectra

The benchmark spectrum for $G^{\bullet+}$ (Fig. 1A) is the same as that shown in Fig. 7B of ref. (*22*), in which dGMP in 8 *M* LiCl containing the electron scavenger $Fe(CN)_6^{3-}$, is oxidized by $Cl_2^{\bullet-}$.

For C(N3)H$^{\bullet}$ (Fig. 1B), the spectrum used is the same as that of Fig. 4D of ref. (*22*), except that wing baseline zeroing was done to eliminate an irregular baseline. The original spectrum was obtained by subtraction of the spectrum for $G^{\bullet+}$ from that of irradiated poly[dG]$^{\bullet}$poly[dC].

For $T^{\bullet-}$ (Fig. 1C), the spectrum shown in Fig. 5B of ref. (*22*) was used, with the exception that the somewhat irregular baseline was set to zero intensity in the wings. This spectrum was derived by electron attachment to TMP in 8 *M* LiCl at 100 K.

The benchmark spectrum (Fig. 1D) used for the putative neutral radicals ($\Sigma N_i^{\bullet}$), was obtained by subtracting $G^{\bullet+}$ as 15% and C(N3)H$^{\bullet}$ as 13% from a spectrum of hydrated DNA ($\Gamma = 14 \pm 2$ D_2O/nucleotide) containing both $K_4Fe(CN)_6$ (1 per 20 bp) and $K_3Fe(CN)_6$ (1 per 20 bp) γ-irradiated with a dose of 12 kGy at 77 K.

The $C3'_{dephos}$ was first described in DNA irradiated with an ^{40}Ar ion beam (*15*). This radical is thought to form through dissociative electron attachment and is thereby not part of the electron-loss path. The spectrum for this radical (Fig. 7C) is simulated using hyperfine and *g*-value parameters close to those from ref. (*15*): $A_{iso}(1H) = 2.69$ mT, $A_{iso}(1H) = 3.46$ mT, $A_{iso}(1H) = 4.75$ mT and $A_{aniso}(1H) = (-1.10, -2.38, -3.40)$ mT, $g = (2.0044, 2.0023, 2.036)$, line width = 0.60 mT. These values provide a slight improvement and minor correction (to the *g* factor) to those in ref. (*15*).

The C3′ sugar radical (Fig. 7D) is described in refs. (*6, 11–13*); the simulation in Fig. 7D uses the hyperfine and *g* values given for the radical in DNA (*6*): $A_{iso}(2H) = 3.0$ mT, $A_{iso}(1H) = 1.7$ mT, $g = (2.0033, 2.0028, 2.0034)$ and line width = 0.50 mT. Using isotopic substitution in guanosine, we have developed compelling evidence that the radical that gives this spectrum, in which the outer line components are separated by 7.7 mT, is the C3′$^{\bullet}$ rather than the C4′$^{\bullet}$ (to be published).

The origin of the benchmark spectrum for the C1′$^{\bullet}$ (Fig. 7E) is given in ref. (*11*).

The spectrum in Fig. 7F is simulated using parameters consistent with a C5′$^{\bullet}$ that possesses a single anisotropic hydrogen hyperfine coupling and a spin density of about 0.85 on the α carbon: $A(1H) = (-0.90, -1.90, -3.00)$ mT, $g = (2.0040, 2.0023, 2.0034)$, and line width = 0.50 mT. The spin density of 0.85 is within the range of spin densities (0.60–0.88) cited by Close for the C5′ carbon in this radical in a variety of model compounds (*27*), and it results in a spectrum that closely matches the approximately 2.1 mT central doublet in Fig. 7B. However, it is conceivable that one or more conformations of the C4′ sugar radical might have a single isotropic coupling of about 2.1 mT which would give a similar, albeit isotropic, doublet. The ESR spectrum for neither the C5′$^{\bullet}$ nor C4′$^{\bullet}$ has been reported in hydrated DNA, to the best of our knowledge. Close has suggested that both of these radicals might yield a doublet for B-form DNA (*27*), although with different hydrogen hyperfine couplings than those proposed here. For $C5'^{\bullet}_{dephos}$, two computer simulations were performed. One used $A(2H) = (-1.06, -2.04, -3.45)$ mT and $A(1H) = 3.6$ mT (*23*) with $g = (2.0038, 2.0023, 2.0034)$ and a 0.70 mT Gaussian linewidth (Fig. 7G, dotted line); the solid spectrum uses the same parameters except that the β-proton coupling to the C4 hydrogen is $A(1H) = 2.0$ mT (Fig. 7G, solid line).

Received: November 10, 2004; accepted: January 6, 2005

REFERENCES

1. D. J. Brenner and C. R. Geard, Links between radiation track structure, radiochemical species and cell survival. In *The Early Effects of Radiation on DNA*, pp. 33–48. NATO ASI Series, Vol. H54, Springer Verlag, Heidelberg, 1991.
2. J. F. Ward, DNA damage produced by ionizing radiation in mammalian cells: Identities, mechanisms of formation and repairability. *Prog. Nucleic Acid Res. Mol. Biol.* **35**, 95–125 (1988).
3. C. Tronche, B. K. Goodman and M. M. Greenberg, DNA damage induced via independent generation of the radical resulting from formal hydrogen abstraction from the C1′-position of a nucleotide. *Chem. Biol.* **5**, 263–271 (1998).
4. W. K. Pogozelski and T. D. Tullius, Oxidative strand scission of nucleic acids: Routes initiated by hydrogen abstraction from the sugar moiety. *Chem. Rev.* **98**, 1089–1107 (1998).
5. W. Wang, M. Yan, D. Becker and M. D. Sevilla, The influence of hydration on the absolute yields of primary free radical in gamma-irradiated DNA at 77 K. II. Individual radical yields. *Radiat. Res.* **137**, 2–10 (1994).
6. B. Weiland and J. Hüttermann, Free radical from X-irradiated dry and hydrated lyophilized DNA as studied by electron spin resonance spectroscopy: Analysis of spectral components between 77K and room temperature. *Int. J. Radiat. Biol.* **74**, 341–358 (1998).
7. J. Hüttermann, M. Roehrig and W. Köhnlein, Free radicals from irradiated lyophilized DNA: Influence of water of hydration. *Int. J. Radiat. Biol.* **61**, 299–313 (1992).
8. S. Gregoli, M. Olast and A. Bertinchamps, Radiolytic pathways in γ-irradiated DNA: Influence of chemical and conformational factors. *Radiat. Res.* **89**, 238–254 (1982).
9. M. D. Sevilla, D. Becker, M. Yan and S. R. Summerfield, Relative abundance of primary radical ions in γ-irradiated DNA: Cytosine vs thymine anions and guanine vs adenine cations. *J. Phys. Chem.* **95**, 3409–3415 (1991).
10. Y. Razskazovskii, M. Roginskaya and M. D. Sevilla, Modification of the reductive pathway in gamma-irradiated DNA by electron scavengers: Targeting the sugar-phosphate backbone. *Radiat. Res.* **149**, 422–432 (1998).
11. L. I. Shukla, R. Pazdro, J. Huang, C. Devreugd, D. Becker and M. D. Sevilla, The formation of DNA sugar radicals from photoexcitation of guanine cation radicals. *Radiat. Res.* **161**, 582–590 (2004).
12. D. Becker, Y. Razskazovskii, M. U. Callaghan and M. D. Sevilla, Electron spin resonance of DNA irradiated with heavy ion beam ($^{16}O^{8+}$): Evidence for damage to the deoxyribose phosphate backbone. *Radiat. Res.* **146**, 361–368 (1996).
13. B. Weiland and J. Hüttermann, Free radicals from lyophilized 'dry' DNA bombarded with heavy ions as studied by electron spin resonance spectroscopy. *Int. J. Radiat. Biol.* **75**, 1169–1175 (1999).
14. M. G. Debije and W. A. Bernhard, Electron paramagnetic resonance evidence for C3′ sugar radical in crystalline d(CTCTCGAGAG) X-irradiated at 4 K. *Radiat. Res.* **155**, 687–692 (2001).
15. D. Becker, A. Bryant-Friedrich, C. Trzasko and M. D. Sevilla, Electron spin resonance study of DNA irradiated with an argon-ion beam: Evidence for formation of sugar phosphate backbone radicals. *Radiat. Res.* **160**, 174–185 (2003).
16. Y. Razskazovskiy, M. G. Debije and W. A. Bernhard, Strand breaks produced in X-irradiated crystalline DNA: Influence of base sequence. *Radiat. Res.* **159**, 663–669 (2003).
17. S. G. Swarts, D. Becker, M. D. Sevilla and K. T. Wheeler, Radiation-induced damage as a function of hydration. II. Base damage from the electron loss centers. *Radiat. Res.* **145**, 304–314 (1996).
18. K. Seiber and J. Hüttermann, Matrix-isolation of H$^{\bullet}$-induced free radicals from purines in acidic glasses. *Int. J. Radiat. Biol.* **55**, 331–345 (1989).
19. Y. Razskazovskiy, M. G. Debije and W. A. Bernhard, Direct radiation damage to crystalline DNA: What is the source of unaltered base release? *Radiat. Res.* **153**, 436–441 (2000).
20. C. von Sonntag, *The Chemical Basis of Radiation Biology*. Taylor & Francis, Philadelphia, 1987.
21. D. Becker and M. D. Sevilla, The chemical consequences of radiation damage in DNA. *Adv. Radiat. Biol.* **17**, 121–180 (1993).
22. W. Wang, D. Becker and M. D. Sevilla, The influence of hydration on absolute yields of primary free radicals in gamma-irradiated DNA at 77 K. I. Total radical yields. *Radiat. Res.* **135**, 146–154 (1993).
23. D. M. Close, E. O. Hole, E. Sagstuen and W. H. Nelson, EPR and

ENDOR studies of x-irradiated single crystals of deoxycytidine 5′-phosphate monohydrate at 10 K and 77 K. *J. Phys. Chem. A* **102**, 6737–6744 (1998).

24. X. Li, M. D. Sevilla and L. Sanche, Density functional theory studies of electron interaction with DNA. Can zero eV electrons induce strand breaks? *J. Am. Chem. Soc.* **125**, 13668–13669 (2003).

25. A-O. Colson and M. D. Sevilla, Ab initio molecular orbital calculations of radicals formed by H· and ·OH addition to the DNA bases: Electron affinities and ionization potentials. *J. Phys. Chem.* **99**, 13033–13037 (1995).

26. F. A. Cotton, G. Wilkinson, C. A. Murillo and M. Bochmann, *Advanced Organic Chemistry*, 6th ed., p. 781. Wiley, New York, 1999.

27. D. M. Close, Where are the sugar radicals in irradiated DNA? *Radiat. Res.* **147**, 663–673 (1997).